LETTERS
PUBLISHED ONLINE: 20 JUNE 2010 | DOI: 10.1038/NNANO.2010.107
nature nanotechnology

Self-assembly of three-dimensional prestressed tensegrity structures from DNA

Tim Liedl[1,2,3†], Björn Högberg[1,2,3], Jessica Tytell[3,4,5,6], Donald E. Ingber[3,4,5,6] and William M. Shih[1,2,3*]

Tensegrity, or tensional integrity, is a property of a structure indicating a reliance on a balance between components that are either in pure compression or pure tension for stability[1,2]. Tensegrity structures exhibit extremely high strength-to-weight ratios and great resilience, and are therefore widely used in engineering, robotics and architecture[3,4]. Here, we report nanoscale, prestressed, three-dimensional tensegrity structures in which rigid bundles of DNA double helices resist compressive forces exerted by segments of single-stranded DNA that act as tension-bearing cables. Our DNA tensegrity structures can self-assemble against forces up to 14 pN, which is twice the stall force of powerful molecular motors such as kinesin or myosin[5,6]. The forces generated by this molecular prestressing mechanism can be used to bend the DNA bundles or to actuate the entire structure through enzymatic cleavage at specific sites. In addition to being building blocks for nanostructures, tensile structural elements made of single-stranded DNA could be used to study molecular forces, cellular mechanotransduction and other fundamental biological processes.

Classic examples of tensegrity structures are the sculptures of Kenneth Snelson, which suspend isolated rigid columns in mid-air by interconnecting them with a continuous tensile cable network that prestresses the whole system (Fig. 1a)[1], and the geodesic domes of Buckminster Fuller that use triangulation and minimal tensional paths between all pairs of neighbouring vertices to maintain their stability[2]. Prestressed tensegrity structures are found at all size scales in living systems[7] and play a central role in cellular mechanotransduction[8]. A number of wireframe structures have been built from DNA[9–13]; however, these are relatively static shapes that do not display many of the novel mechanical features of prestressed tensegrity structures, such as the ability to globally reorient internal members and thereby strengthen in response to a local stress. Here, we set out to use the DNA-origami method[14,15] to build prestressed tensegrity structures on the nanoscale that exhibit integrated mechanical responses similar to those displayed by living cellular systems.

To accomplish this goal, we moved beyond the current DNA-origami methods used to create nanostructures, which rely only on paired bases to provide structural integrity. Instead, we incorporated stretched single-stranded DNA (ssDNA) segments as nanoconstruction elements that act in solution as entropic springs, the behaviour of which can be described over a wide range of loads using a modified freely jointed chain model (mFJC) that accounts for stretchable Kuhn segments[16] (Supplementary Note S9). We designed and fabricated prestressed DNA tensegrity structures consisting of a 8,634-nucleotide (nt) M13mp18-based 'scaffold strand' and hundreds of oligodeoxyribonucleotide 'staple strands' that self-assemble into tensed structures despite kinetic barriers imposed by the prestress. The assembly process for prestressed origami objects is, as for DNA-origami objects in general, a one-pot reaction where the scaffold strand, the staple strands and buffer containing Mg^{2+} ions are heated to 80 °C and then cooled down over the course of 72 h to room temperature to allow each staple strand to find its unique position on the scaffold sequence and hence achieve the correct assembly of the structure. The staple sequences were designed, using the software caDNAno (ref. 17), to promote self-assembly of rigid columns or struts composed of bundles of multiple DNA double helices. Importantly, this design differed from those used for previously reported DNA-origami structures because we also incorporated loops of hundreds of unpaired bases on the scaffold strand that connect the ends of multiple individual struts and act as the ssDNA springs. Two stretches of the scaffold DNA for which the sequences are prone to hairpin formation were incorporated into the rigid struts. A simplifying assumption of our model is that secondary-structure formation in the ssDNA springs can be ignored. Future experiments could use structure-free ssDNA (for example, scaffold segments programmed to consist primarily of the bases A, C and T) as the springs to make this assumption more valid. The energy necessary for tightening of these ssDNA springs is provided during the assembly process by base-pairing of the double helices that form the compression-resistant struts, thereby prestressing the entire integrated DNA structure.

As a proof-of-principle for this strategy, we designed a three-dimensional 'tensegrity prism' composed of three compression-resistant, 57-nm-long, 13-helix bundles held in place by nine tensed ssDNA springs (each 226 bases long) (Fig. 1b,c). Each strut was constructed from three segments of the scaffold that were far apart in the primary sequence, providing five, three and five of the 13 helices, respectively (Fig. 1d). Transmission electron microscopic (TEM) analysis of gel-purified structures self-assembled in this manner, and comparison of these two-dimensional images with predicted three-dimensional computer models, confirmed that this self-assembly process resulted in three-strut tensegrity prisms (Fig. 1e; see also Supplementary Fig. S1), and similar results were obtained by constructing another tensegrity prism using six-helix bundles as struts (Supplementary Fig. S2).

With a view to investigating the influence of ssDNA spring length, and thus tension, on the structure and assembly success of DNA tensegrity structures, we created a two-dimensional, prestressed 'kite' structure (Fig. 2a). The ends of two 92-nm-long, 12-helix bundles were connected through four unpaired regions of

[1]Department of Cancer Biology, Dana-Farber Cancer Institute, Harvard Medical School, Boston, Massachusetts 02115, USA, [2]Department of Biological Chemistry and Molecular Pharmacology, Harvard Medical School, Boston, Massachusetts 02115, USA, [3]Wyss Institute for Biologically Inspired Engineering at Harvard University, Cambridge, Massachusetts 02138, USA, [4]Vascular Biology Program, Children's Hospital, Harvard Medical School, Boston, Massachusetts 02115, USA, [5]Department of Pathology, Harvard Medical School, Boston, Massachusetts 02115, USA, [6]Harvard School of Engineering and Applied Sciences, Cambridge, Massachusetts 02138, USA; †Present address: Center for Nanoscience, CeNS, Ludwig-Maximilians-Universität, Fakultät für Physik, Geschwister Scholl Platz 1, D-80539, München, Germany. *e-mail: William_Shih@dfci.harvard.edu

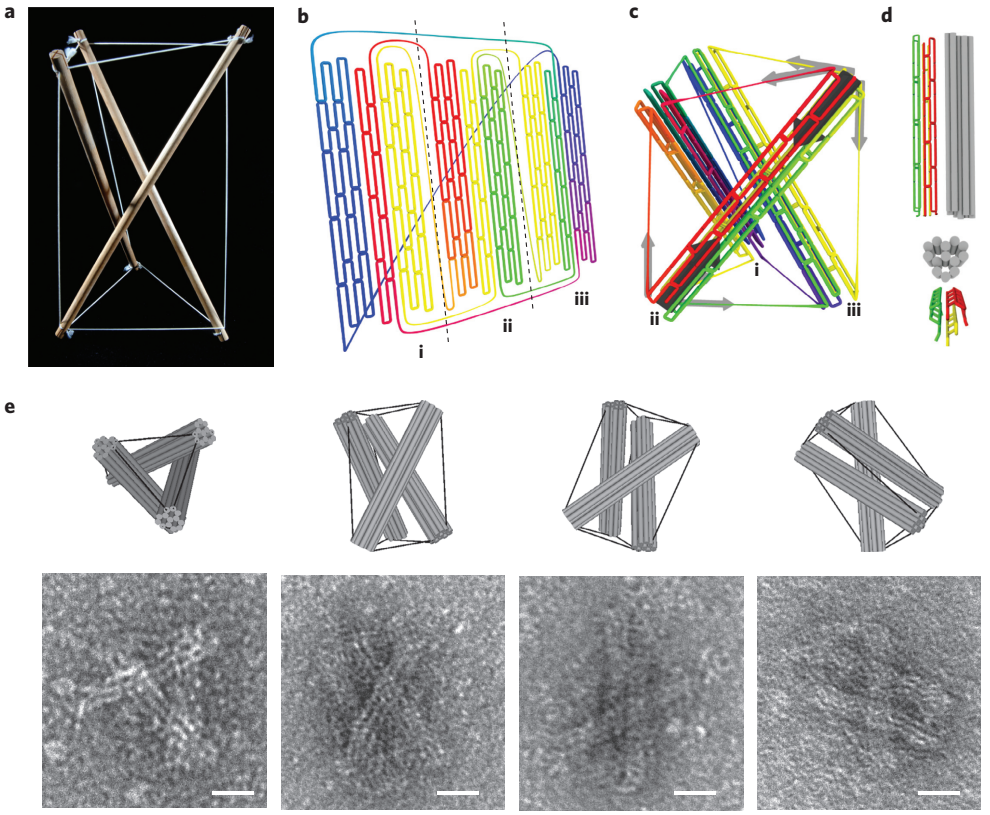

Figure 1 | Three-dimensional prestressed DNA tensegrity. a, Tensegrity prism constructed from wood and cord. **b**, Quasi-two-dimensional representation of the scaffold pathway through the prestressed tensegrity prism. The colour code indicates the nucleotide (nt) index along the circular path. Red represents the first nt on the 8,634-nt-long scaffold, violet the last nt. The three struts are labelled i, ii, iii. **c**, Three-dimensional representation of the scaffold pathway for the assembled prism. Staple strands are omitted for clarity. Light grey arrows denote the contractile forces exerted by the ssDNA springs, and dark grey arrows indicate the sum of compressive forces along the axis of the 13-helix bundle. **d**, Cylinder and scaffold models of an individual 13-helix bundle. Every cylinder represents one double helix. **e**, Electron micrographs and cylinder models of DNA tensegrity prisms. Scale bars, 20 nm.

a 8,634-nt scaffold strand; no DNA strands cross over between the two 12-helix bundles at the point of intersection. Hence, the structural integrity is solely provided by the tension of the four DNA springs, balanced by the compression imposed on the struts to which they connect. In a perfect square arrangement, the distances between pairs of neighbouring ends of the struts are each 65 nm. Stretched over this distance in solution at room temperature, an idealized ssDNA spring of 220 nt exerts a contractile force between 6 and 7 pN. We calculated the force with two models that estimate extension–force relations for polymers in solution: the mFJC model (6.4 pN) and the wormlike chain (WLC) model[18], which implies continuous bending elasticity (6.9 pN) (Supplementary Fig. S3, Supplementary Notes S9–11). To investigate the structural rigidity and the maximum force achievable with this approach, the kite structure was assembled in nine configurations with spring lengths of 520, 420, 320, 220, 190, 170, 160, 150 and 140 nt. The different numbers of bases in the single-stranded regions were achieved by exchanging a small subset of staple strands, which led to spooling of the desired number of unused bases. The enlarged schematics in Fig. 2a show the scaffold and staple paths at the end of a 12-helix bundle before and after spooling.

Sample analysis by gel electrophoresis after annealing resulted in a series of bands (Fig. 2b). The second fastest band contained structures with the desired kite configuration, in which shorter spring lengths led to tighter distributions of crossing angles β (Fig. 2b, lower panel). The red lines overlaying the histograms represent the equilibrium angle distributions at room temperature calculated from the mFJC model (for a WLC model fit, see Supplementary Fig. S3). The next slower migrating band was composed of dimers, that is, two sets of staple strands sharing two scaffold strands. With spring lengths that generate forces greater than 14 pN (160 nt), no desired kite structures formed, indicating that a 12-helix bundle can fold into its full length against forces up to 14 pN acting on each end. However, the yield of correctly folded objects for this particular geometry was highest (~15% efficiency) at forces between 4 and 7 pN (320 and 220 nt, respectively).

In all lanes, we detected a faint fast-moving lowermost band that contained objects with a parallel arrangement of the two struts when visualized using TEM. We attribute these defective particles to the occasional rupturing of the scaffold strand in one of the four springs. We were also able to mechanically actuate this structural transition between a square-kite configuration to the parallel conformation in a controlled manner, and with high efficiency, by clipping specific sites in the springs with a restriction endonuclease. After clipping, the band of the kite in a square arrangement disappeared, and the band for the struts arranged in parallel gained intensity (Fig. 2c).

To demonstrate the versatility of prestressed DNA tensegrity structures, a geometrical variant of the kite was designed and nanofabricated through self-assembly. One of the four springs was fixed to a length of 140 nt, and the remaining three springs were set with a length of 320 nt (Fig. 2d). Interestingly, when we engineered similar structures using thinner, 128-nm-long, six-helix bundles[19] as compression-resistant elements, we observed buckling of these struts (Fig. 3; see also Supplementary Fig. S5). Introducing shorter 42-nt-long six-helix bundle segments into each spring, the ssDNA length between the ends of a six-helix-bundle kite structure was fixed at 486 bases. After thermal annealing, gel purification and

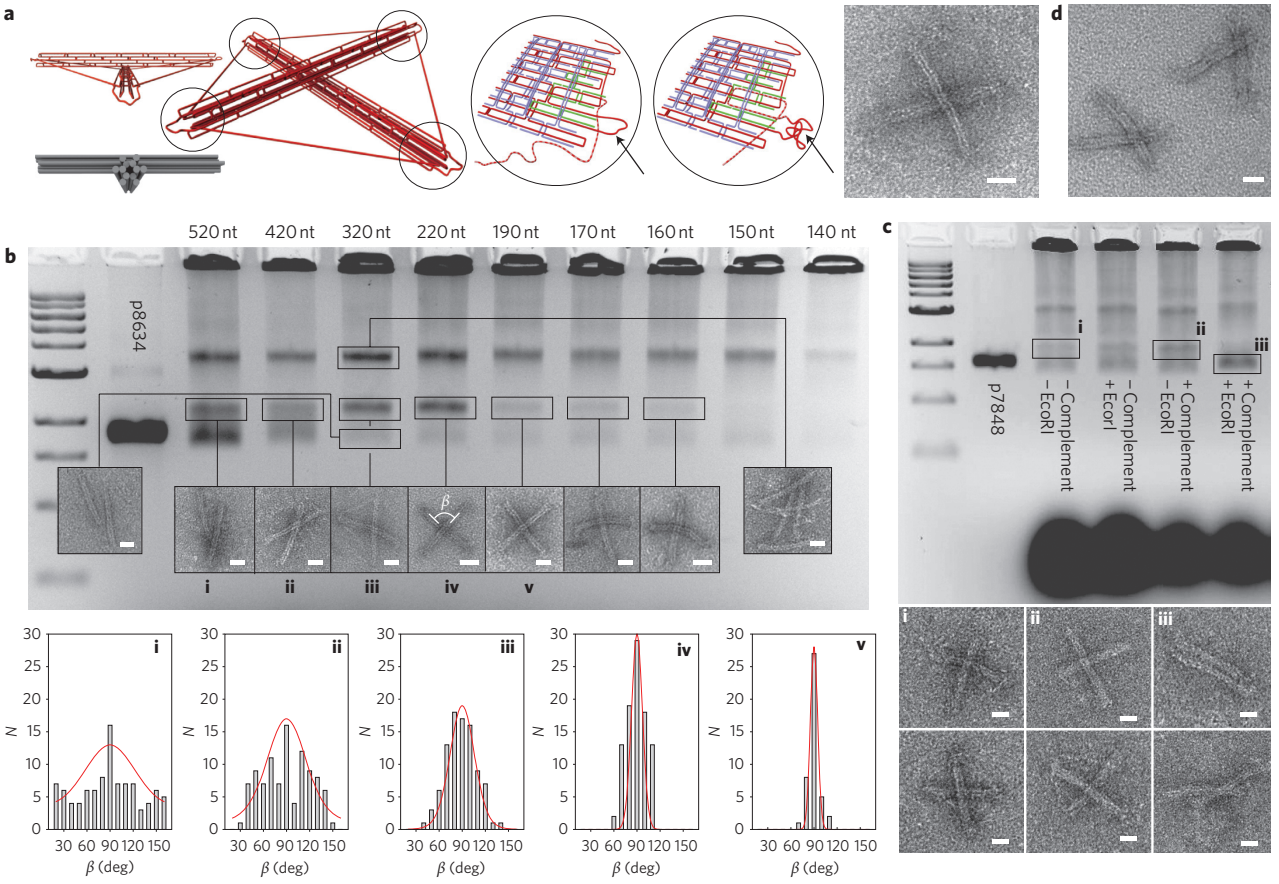

Figure 2 | DNA tensegrity-structure kite. a, Three-dimensional scaffold path representation for the prestressed tensegrity kite and TEM image of the assembled object with 220-nt-long springs. Changes of the spring lengths of a DNA tensegrity structure can be achieved by spooling of the scaffold DNA. Staple strands that have to be exchanged to achieve a shortening of a spring are depicted in green. **b**, Gel and TEM analysis of kites equipped with varying spring lengths between the ends of the struts. Left to right: 2-Log DNA ladder, p8634 scaffold, 520 nt, 420 nt, 320 nt, 220 nt, 190 nt, 170 nt, 160 nt, 150 nt, 140 nt. The bands containing the various objects were extracted and investigated with TEM. Lower panels: histograms of observed angles β between the struts. **c**, A 12-helix-bundle kite with four springs of equal length (300 nt) was designed such that the restriction site for EcoRI was located in one of the 300-nt-spring regions. Gel (top) and TEM analysis (bottom panels) shows that the enzymes only cut the springs when the complementary sequence to the restriction site is present during folding. Species cut out of gel and analysed by TEM are indicated as i, ii and iii. **d**, TEM image of kites with one short spring (140 nt) and three longer springs (320 nt). Scale bars, 20 nm.

TEM imaging, most of these objects displayed two bent six-helix bundles, which can be explained as follows. The critical force F_c at which a strut of length L buckles can be expressed as $F_c = \pi^2 \cdot P \cdot k_B T / L^2$. If we assume a persistence length of $P = 1.6 \pm 0.6$ μm for our gel-purified six-helix bundles (see next paragraph and Supplementary Fig. S5), $F_c = 3.9 \pm 1.5$ pN. Because the expected force exerted by the ssDNA on the straight struts of 4.7 ± 1 pN is above this critical force, the buckling of the six-helix bundles is not surprising. The mean distance d between ends of neighbouring struts on the TEM grid was 72 ± 9 nm, which corresponds to an average force of 2.5 ± 0.5 pN along each spring. These forces sum to a resulting force of 3.5 ± 1 pN along the axis of each strut, which coincides, within error margins, with the predicted critical buckling force of 3.9 ± 1.5 pN. The measured distances and the resulting forces are estimated under the simplifying assumptions that our DNA objects adhere to the grids without further equilibrating movements during drying and staining and that the restoring force of a buckling strut is constant. We are therefore ignoring effects of a potentially damaged or distorted cross-section of the strut.

We also determined that our six-helix bundles have a persistence length of 2.4 ± 0.6 μm, which agrees well with the theoretically expected value of 2.7 μm (Supplementary Figs S6,S7). For six-helix bundles purified from an agarose gel, the measured persistence length drops to 1.6 ± 0.6 μm, most likely due to incorporation of ethidium bromide (Supplementary Fig. S8) and mechanical damage during gel electrophoresis and extraction (Supplementary Fig. S8). Consistent with the observation that gel purification lowers the persistence length, we found that unpurified six-helix-bundle kites exhibit straight struts, and therefore display an average distance of 89 ± 3 nm between neighbouring strut ends (Supplementary Fig. S4). Hence, unpurified, 128-nm, six-helix bundles that experience a compression force of 4.7 ± 1 pN do not buckle. This observation is consistent with theory, because a force greater than 6 pN is required to buckle unpurified six-helix bundles of this length, with a persistence length of 2.4 μm. Thus our results are roughly consistent with the mFJC model for ssDNA and a compressive Young's modulus for dsDNA of 3×10^8Pa (refs 20,21). In the future, more complex models (for example, one that considers the ionic strength of the solution) might yield a more complete picture and will have to be used in the low-force regime (<2 pN) to obtain accurate predictions[22]. However, the active bending of DNA-origami objects provides a visual demonstration of our ability to generate controllable forces during the process of DNA self-assembly. By applying known nanoscale forces by means of this structural approach, it might be possible to quantitatively probe and analyse biophysical mechanisms at the molecular level in the future.

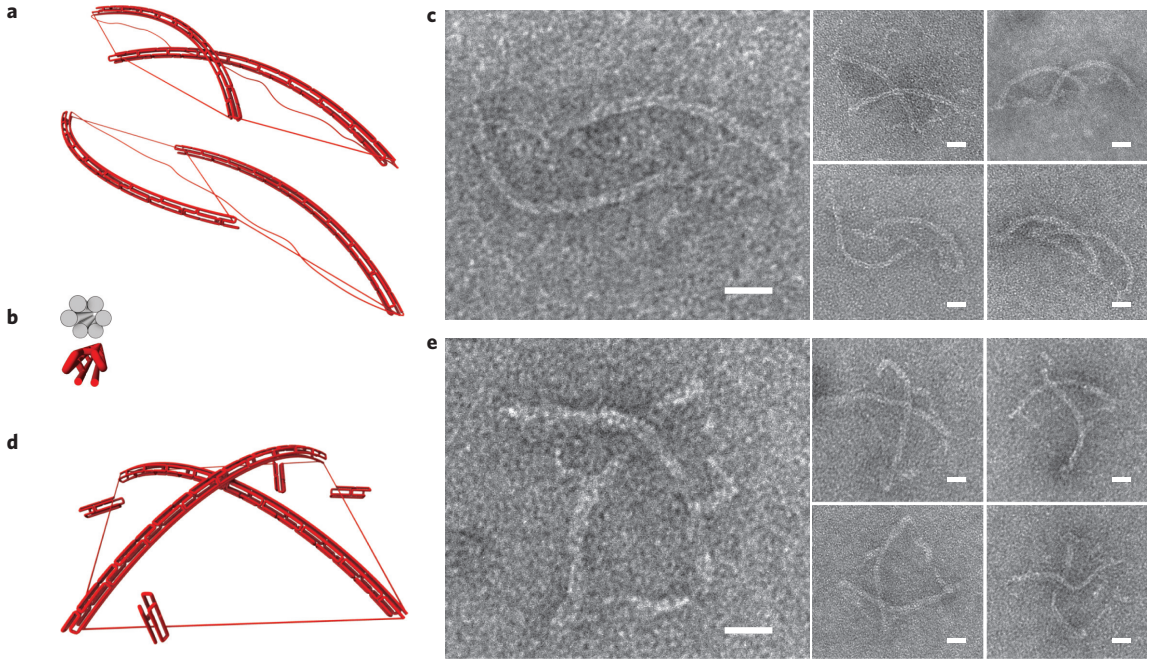

Figure 3 | Force generation with DNA tensegrity objects. Six-helix bundles under compression buckle if the compressive force exceeds the critical Euler force F_c. **a**, Models of distorted tensegrity kites with 128-nm-long six-helix-bundle struts, three short ssDNA springs that are 273 nt long, and a long fourth spring that is 2,207 nt long. **b**, Profiles of the design of the struts, cylinder model and scaffold path representation. **c**, TEM images of gel-purified objects of the type shown in **a. d**, Model of a buckling kite with four springs of equal length (486 nt each, length adjusted with four six-helix-bundle clamps). **e**, TEM micrographs of gel-purified buckling kites. By measuring the end-to-end distance of multiple six-helix bundles as in **c** and **e**, the resultant force acting on the six-helix-bundle ends could be estimated to be 4 pN. Equating the obtained value with F_c leads to an estimated persistence length P of the six-helix bundle of 1.4 μm. This is in good agreement with the value of P obtained for gel-purified, ethidium-bromide-soaked six-helix bundles by independent measurements (Supplementary Fig. S7). Scale bars, 20 nm.

Application of ssDNA as spring elements in DNA structures could give rise to the fabrication of flexible and mechanically responsive DNA structures spanning great areas or volumes while using relatively small amounts of material. Current efforts to use dsDNA as a scaffold source[23], and the potential of hierarchical assembly[12,15], may facilitate the creation of such large biocompatible constructs. We have shown that the inclusion of specific cleavage sequences in the DNA sequence enables ligand-inducible mechanical actuation. In combination with the coupling of aptamer-based enzymatic activity into DNA tensegrity structures, this could provide a mechanism to generate mechanochemical conversion mechanisms similar to those observed in living cells[8], which might be useful in the origin of life studies to model hierarchical, self-assembling, tensegrity structures that have been proposed to contribute to the emergence of the first living cells[24]. These programmable biomimetic nanostructures could be used as nanoscale solution-based force sensors[25] and as platforms for biophysical experiments where DNA of defined length under controlled tension is desirable. Furthermore, they could serve as artificial extracellular matrices with controllable mechanics or as cytoskeletal-network mimics that could aid in the study of fundamental cellular processes such as cellular mechanotransduction, which involves stress-dependent control of molecular biochemistry and gene expression.

Methods

Folding and purification of prestressed DNA tensegrity structures. For the self-assembling process, a solution containing 10 nM of scaffold strand, 50 nM of each staple strand (reverse-phase cartridge purified; Bioneer), 5 mM Tris + 1 mM EDTA (pH 7.9 at 20 °C), 16 mM $MgCl_2$ was heated to 80 °C for 4 min, cooled to 60 °C over the course of 80 min, and cooled further to 24 °C over the course of 72 h. The folded objects were electrophoresed on a 1.5% agarose gel containing 45 mM Tris borate + 1 mM EDTA and 11 mM $MgCl_2$ at 70 V for 3 h. To protect the origami structures from denaturation during electrophoresis, the gel-box was cooled in an ice-water bath. The gel band containing the structures was physically extracted from the gel and run through spin columns (Freeze'n'Squeeze Spin Columns, Biorad) at 5,000 *g*. The DNA tensegrity objects were then imaged with TEM after negative staining with uranyl formate on a FEI Tecnai T12 BioTWIN at 80 kV.

Ligand-induced mechanical actuation of the 12-helix-bundle kite. A 12-helix-bundle kite with four springs of equal length (300 nt) was designed such that the restriction site for EcoRI was located in one of the 300-nt-spring regions. The assembled kites with a double-stranded region at the EcorRI restriction site (GAATTC + 10 bases or more overhang on both sides of the sequence) were incubated for 1 h with the enzymes (20 μl of 10 nM scaffold, 80 nM each staple, 1 × NEB-buffer 2, 20 units of enzyme, New England Biolabs). Uncut and cut tensegrity kites were electrophoresed on a 1.5% agarose gel. The gel bands were physically extracted and imaged with TEM after negative staining with uranyl formate.

Received 13 November 2009; accepted 30 April 2010; published online 20 June 2010

References

1. Snelson, K. Snelson on the tensegrity invention. *Int. J. Space Struct.* **11,** 43–48 (1996).
2. Fuller, B. *Synergetics—Explorations in the Geometry of Thinking* Vols I and II (Macmillan Publishing, 1975, 1979).
3. Skelton, R. E., Adhikari, R., Pinaud, J. P. & Chan, W. An introduction to the mechanics of tensegrity structures. *Proceedings of the 40th IEEE Conference on Decision and Control* **5,** 4254–4259 (2001).
4. Sultan, C. Corless, M. & Skelton, R. E. The prestressabilty problem of tensegrity structures: some analytical solutions. *Int. J. Solids Struct.* **38,** 5223–5252 (2001).
5. Visscher, K., Schnitzer, M. J. & Block, S. M. Single kinesin molecules studied with a molecular force clamp. *Nature* **400,** 184–189 (1999).
6. Clemen, A. E. *et al.* Force-dependent stepping kinetics of myosin-V. *Biophys. J.* **88,** 4402–4410 (2005).
7. Ingber, D. E. The architecture of life. *Sci. Am.* **278,** 48–57 (1998).
8. Ingber, D. E. Cellular mechanotransduction: putting all the pieces together again. *FASEB J.* **20,** 811–827 (2006).
9. Shih, W. M., Quispe J. D. & Joyce, G. F. A 1.7-kilobase single-stranded DNA that folds into a nanoscale octahedron. *Nature* **427,** 618–621 (2004).

10. Liu, D., Wang, M. S., Deng, Z. X., Walulu, R. & Mao, C. D. Tensegrity: construction of rigid DNA triangles with flexible four-arm DNA junctions. *J. Am. Chem. Soc.* **126,** 2324–2325 (2004).
11. Zhang, C. *et al.* Conformational flexibility facilitates self-assembly of complex DNA nanostructures. *Proc. Natl Acad. Sci.* **31,** 10665–10669 (2008).
12. He, Y. *et al.* Hierarchical self-assembly of DNA into symmetric supramolecular polyhedra. *Nature* **452,** 198–201 (2008).
13. Zheng, J. *et al.* From molecular to macroscopic via the rational design of a self-assembled 3D DNA crystal. *Nature* **461,** 74–77 (2009).
14. Rothemund, P. W. K. Folding DNA to create nanoscale shapes and patterns. *Nature* **440,** 287–302 (2006).
15. Douglas, S. M. *et al.* Self-assembly of DNA into nanoscale three-dimensional shapes. *Nature* **459,** 414–418 (2009).
16. Smith, S. B., Cui, Y. J. & Bustamante, C. Overstretching B-DNA: the elastic response of individual double-stranded and single-stranded DNA molecules. *Science* **271,** 795–799 (1996).
17. Douglas, S. M. *et al.* Rapid prototyping of three-dimensional DNA-origami shapes with caDNAno. *Nucleic Acids Res.* **37,** 5001–5006 (2009).
18. Marko, J. F. & Siggia, E. D. Stretching DNA. *Macromolecules* **28,** 8759–8770 (1995).
19. Douglas, S. M., Chou, J. J. & Shih, W. M. DNA-nanotube-induced alignment of membrane proteins for NMR structure determination. *Proc. Natl Acad. Sci. USA* **104,** 6644–6648 (2007).
20. Howard, J. *Mechanics of Motor Proteins and the Cytoskeleton* (Sinauer Associates, 2001).
21. Goodman, R. P. *et al.* Rapid chiral assembly of rigid DNA building blocks for molecular nanofabrication. *Science* **310,** 1661–1665 (2005).
22. Saleh, O. A., McIntosh, D. B., Pincus, P. & Ribeck, N. Nonlinear low-force elasticity of single-stranded DNA molecules. *Phys. Rev. Lett.* **102,** 068301 (2009).
23. Högberg, B., Liedl, T. & Shih, W. M. Folding DNA origami from a double-stranded source of scaffold. *J. Am. Chem. Soc.* **131,** 91544–94155 (2009).
24. Ingber, D. E. The origin of cellular life. *Bioessays* **22,** 1160–1167 (2000).
25. Shroff, H. *et al.* Biocompatible force sensor with optical readout and dimensions of 6 nm^3. *Nano Lett.* **5,** 1509–1514 (2005).

Acknowledgements

The authors thank O. Hallatschek, R. Neher, H. Dietz and S. Douglas for helpful discussions and advice. This work was funded by the Wyss Institute for Biologically Inspired Engineering, and Deutscher Akademischer Austauschdienst (DAAD; T.L.), Swedish Science Council (Vetenskapsrådet) Fellowship (B.H.) and Claudia Adams Barr Program Investigator and NIH New Innovator (1DP2OD004641-01; W.M.S.) grants.

Author contributions

T.L., D.E.I. and W.M.S. conceived and designed the research. T.L. designed the DNA shapes. T.L., B.H. and J.T. performed the experiments. T.L. and B.H. analysed the data, and T.L., B.H., D.E.I. and W.M.S. co-wrote the paper.

Additional information

The authors declare no competing financial interests. Supplementary information accompanies this paper at www.nature.com/naturenanotechnology. Reprints and permission information is available online at http://npg.nature.com/reprintsandpermissions/. Correspondence and requests for materials should be addressed to W.M.S.